Multiple-Valued Quantum Logic

Anas Al-Rabadi, Lee Casperson, Marek Perkowski, and Xiaoyu Song
Portland State University
Department of Electrical and Computer Engineering
1900 S.W. 4th Avenue, Portland, OR 97207 U.S.A.
[alrabadi,lcaspers,mperkows,song@ece.pdx.edu]

Abstract

This paper introduces the concept of multiple-valued quantum logic, where more than two quantum basis states are introduced, for instance $\{|0\rangle, |1\rangle, |2\rangle\}$ for ternary quantum logic. Since the binary 2-qubit Einstein-Podolsky-Rosen (EPR) basis states play an important role in quantum logic circuits and superdense coding, their generalization to multiple-valued N-qubit EPR basis states is interesting to be considered, especially that multiple-valued quantum logic is physically feasible. The multiple-valued EPR basis states are achieved by utilizing the new quantum Chrestenson operator, which is also presented in this work. New multiple-valued Galois-field quantum primitives, evolution processes, and the corresponding canonical quantum decision trees and decision diagrams are also introduced as their representations.

1. Introduction

Quantum computing is expected to play an increasingly important role in building more compact and less power-consuming computers [5,7,8,10,11,13,15,16]. The importance of quantum computing stems from the following facts: (1) while transforming highly complex problems from the real domain to other domains (like Fourier domain, Walsh domain, etc) does not reduce the problem complexity, transforming such complex problems to the quantum domain can reduce the problem complexity. Due to this fact, some problems that are not solvable in polynomial time in classical non-quantum domains may be solvable in polynomial time in the quantum domain [16], (2) Quantum logic (QL) permits intensive parallel computations, (3) There are no physical limits to build multiple-valued rather than two-valued quantum gates, and there are arguments for higher efficiency of multiple-valued quantum systems [15], and (4) The requirement of reversible algorithms and codes on quantum machines, thus very little power will be needed (theoretically zero).

So far, not much has been published on multiple-valued quantum logic gates and especially their characterization and representation formalisms. It is the main goal of this paper to start building a systematic theory of multiple-valued quantum gates, structures, and synthesis methods. This paper introduces the following new results:

(1) New multiple-valued primitives and evolution processes.
(2) New multiple-valued Einstein-Podolsky-Rosen basis states.
(3) Generalized multiple-valued quantum permuters.
(4) Multiple-valued canonical quantum decision trees (**QDTs**) and decision diagrams (**QDDs**).

Items 1 and 3 are necessary for automated analysis and verification of netlists of quantum gates. They are also necessary for automated synthesis of a netlist described as an evolution matrix from quantum gates, especially for try-and-check methods such as evolutionary computations [19]. Since decision diagrams [6,18] allow for efficient representation of large sparse matrices, they found applications in many computer aided design (CAD) algorithms, and we believe that their quantum counterparts will be useful for quantum logic synthesis and analysis. Finally, item 2 is important because new forms of quantum decision trees and diagrams can be produced for the new multiple-valued EPR basis states, and thus allowing for further possible optimizations in the design of quantum circuits, analogous to the classical (non-quantum) case where different forms of decision trees and diagrams lead to different scales of optimizations in the design of logic circuits [18].

The remainder of this paper is organized as follows: Background and preliminaries are included in section 2. Multiple-valued quantum primitives, basis states, and canonical representations are presented in section 3. Conclusions and future work are presented in section 4.

2. Background

This section presents the necessary background and preliminaries in order to provide the reader with motivations for the new results that will be presented in section 3.

2.1. Reversible Logic

A (k,k) reversible circuit is a circuit that has the same number of inputs (k) and outputs (k) and is one-to-one mapping between vector of inputs and outputs. Thus, the vector of input values can always be uniquely reconstructed from the vector of output values [1,2,3,4,5,10,11,12,13]. Many reversible gates have been proposed as building blocks for reversible and quantum computing [1,2,3,4,10,12]. Figure 1 shows some of the binary reversible gates that are commonly used in the synthesis of reversible logic circuits.

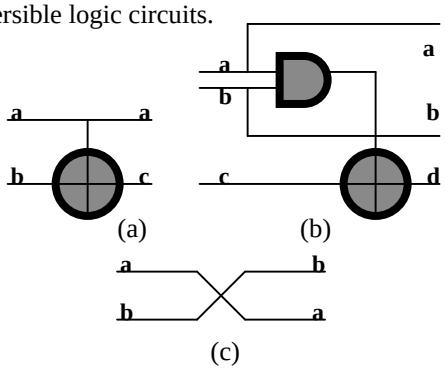

Figure 1. Binary reversible gates: (a) (2,2) Feynman gate, (b) (3,3) Toffoli gate, and (c) (2,2) swap gate.

2.2. Two-Valued Quantum Logic

Quantum logic is a direction in modern computing that utilizes the results of quantum mechanics to perform logic computing using various properties of atomic structures [15,16]. The following definitions are needed to understand the underlying processes of quantum computing, where we follow the standard notation from [9].

Definition 1. A binary quantum bit, or qubit, is a binary quantum system, defined over the Hilbert space H_2 with a basis $\{|0\rangle, |1\rangle\}$.

Definition 2. In binary quantum logic system, qubit-0 and qubit-1 are defined as follows:

$$qubit-0 \equiv |0\rangle = \begin{bmatrix} 1 \\ 0 \end{bmatrix} \Rightarrow spin-up(\uparrow 90^0),$$

$$qubit-1 \equiv |1\rangle = \begin{bmatrix} 0 \\ 1 \end{bmatrix} \Rightarrow spin-down(\downarrow 270^0)$$

In quantum computing each quantum state is considered to be a superposition of primitive states [9,10,16]. Thus, the state of the quantum system is expressed as a linear combination of basis states, i.e. $\alpha_1|x_1\rangle + \alpha_2|x_2\rangle + ... + \alpha_n|x_n\rangle$. The complex-valued amplitudes α_i are referred to as "probability amplitudes" [16] with respect to the basis $\{|x_1\rangle, |x_2\rangle, ..., |x_n\rangle\}$. Quantum computing requires the following constraints that distinguish it from classical computing:

(1) Operations are done on complex vectors of bits called qubits (quantum bits). Qubits are complex-weighted linear superpositions of orthonormal basis states. Some of the basis states that are used in a 1-qubit binary quantum systems include [16]: the computational basis states $\{|0\rangle, |1\rangle\}$, and the basis states $\left\{|+\rangle = \frac{|0\rangle + |1\rangle}{\sqrt{2}}, |-\rangle = \frac{|0\rangle - |1\rangle}{\sqrt{2}}\right\}$. Some of the basis states that are used in a 2-qubit binary quantum systems include [16]: Einstein-Podolsky-Rosen (EPR) basis states $\left\{\frac{|00\rangle + |11\rangle}{\sqrt{2}}, \frac{|00\rangle - |11\rangle}{\sqrt{2}}, \frac{|01\rangle + |10\rangle}{\sqrt{2}}, \frac{|01\rangle - |10\rangle}{\sqrt{2}}\right\}$, and the computational basis states $\{|00\rangle, |01\rangle, |10\rangle, |11\rangle\}$.

(2) Reversible computations, algorithms, and circuits [5,10,11,13].

(3) Unitary operations. These operations are performed in n-dimensional Hilbert space, which is in general a linear complex vector space [9,16].

(4) The quantum register, which is an array of qubits, can be in any of the individual states of its qubits at any instant of time or at all of the states at the same time, thus allowing for *parallelism* at the quantum level [16].

An n-qubit binary quantum register (also called as scratchpad register [10,11]) is a vector of n binary qubits. For a quantum register that is composed of 2 binary qubits, one obtains 4 possible states of the register. These states are as follows:

$$|00\rangle = |0\rangle \otimes |0\rangle = \begin{bmatrix} 1 \\ 0 \end{bmatrix} \otimes \begin{bmatrix} 1 \\ 0 \end{bmatrix} = [1 \quad 0 \quad 0 \quad 0]^T,$$

$$|01\rangle = |0\rangle \otimes |1\rangle = \begin{bmatrix} 1 \\ 0 \end{bmatrix} \otimes \begin{bmatrix} 0 \\ 1 \end{bmatrix} = [0 \quad 1 \quad 0 \quad 0]^T,$$

$$|10\rangle = |1\rangle \otimes |0\rangle = \begin{bmatrix} 0 \\ 1 \end{bmatrix} \otimes \begin{bmatrix} 1 \\ 0 \end{bmatrix} = [0 \quad 0 \quad 1 \quad 0]^T,$$

$$|11\rangle = |1\rangle \otimes |1\rangle = \begin{bmatrix} 0 \\ 1 \end{bmatrix} \otimes \begin{bmatrix} 0 \\ 1 \end{bmatrix} = [0 \quad 0 \quad 0 \quad 1]^T.$$

Where ⊗ is the tensor (Kronecker) product [16]. In general, a binary quantum register that is composed of k binary qubits can have up to 2^k possible states. The quantum register can be in any of the individual states at any instant of time or at all of the states at the same time. For a register composed of 1 qubit, the quantum evolution state $|\Psi\rangle$ is represented as follows [16]:

$$|\Psi\rangle_{binary-qubit} = \sqrt{p_0}|0\rangle + \sqrt{p_1}|1\rangle = \alpha|0\rangle + \beta|1\rangle \quad (1)$$

Where p_0 is the probability of the qubit being in state |0>, and p_1 is the probability of the qubit being in state |1>, and $|\alpha|^2 + |\beta|^2 = p_0 + p_1 = 1$. Equation (1) can be written as:

$$|\Psi\rangle_{binary-qubit} = \begin{bmatrix} |0\rangle & |1\rangle \end{bmatrix} [E] \begin{bmatrix} \alpha \\ \beta \end{bmatrix} \quad (2)$$

where [E] is an evolution matrix. For a quantum register that is composed of many binary qubits, the quantum evolution state is produced using the tensor product.

According to the principles of quantum mechanics, the combination of quantum state qubits can be in either decomposable or in entangled states [16]. While each individual state qubit can be observed in the former case, the same is impossible in the later. The combination of two systems with the bases $\{|x_1\rangle, |x_2\rangle, ..., |x_n\rangle\}$ and $\{|y_1\rangle, |y_2\rangle, ..., |y_m\rangle\}$ is described as a pair $(|x_i\rangle, |y_j\rangle)$, and the composite quantum state is expressed as:

$$\sum_{i=1}^{n}\sum_{j=1}^{m} \alpha_{ij} |x_i, y_j\rangle \quad (3)$$

In quantum logic, one defines a state to be decomposable if it can be expressed as:

$$\sum_{i=1}^{n}...\sum_{j=1}^{m} \alpha_{i...j} |x_i, ..., x_j\rangle = \sum_{i=1}^{n}...\sum_{j=1}^{m} \alpha_i ... \beta_j |x_i\rangle ... |x_j\rangle$$
$$= \sum_{i=1}^{n} \alpha_i |x_i\rangle \otimes ... \otimes \sum_{j=1}^{m} \beta_j |x_j\rangle$$
$$= \sum_{i=1}^{n} \alpha_i |x_i\rangle ... \sum_{j=1}^{m} \beta_j |x_j\rangle \quad (4)$$

Otherwise, the state is entangled. The speedups in quantum computations are seemed to be due to the entanglement, by which many computations are performed in parallel [16]. Various quantum evolution processes that correspond to quantum gates have been introduced [2,10,11].

3. Multiple-Valued Quantum Logic

This section introduces new concepts in multiple-valued quantum logic: multiple-valued quantum primitives, evolution processes, and the corresponding canonical quantum decision trees and decision diagrams as their representations. Since Galois-field was proven to possess attractive properties in testing [17], and quantum error-correction codes [7], the Galois-field algebraic structure will be our fundament for constructing a unified approach to multiple-valued quantum logic.

	0	1	2
0	0	1	2
1	1	2	0
2	2	0	1

(a)

	0	1	2
0	0	0	0
1	0	1	2
2	0	2	1

(b)

Figure 2. (a) Ternary Galois-field addition, and (b) ternary Galois-field multiplication.

Although the results that are presented in the following sections are for the ternary case, generalization to higher radices is straightforward.

3.1. Quantum Chrestenson Gate, and the New Multiple-Valued Einstein-Podolsky-Rosen Basis States

In ternary quantum logic, the "0", "1", and "2" qubits are represented by the vector that corresponds to the spin of atomic particles as shown in Figure 3. The following are basic definitions for a ternary quantum logic system (extensions to any N-ary quantum logic is straightforward).

Definition 3. A ternary quantum bit is a ternary quantum system, defined over the Hilbert space H_3 with a basis $\{|0\rangle, |1\rangle, |2\rangle\}$.

Definition 4. In a ternary quantum logic system, qubit-0, qubit-1, and qubit-2 are defined as follows, respectively:

$$|0\rangle = \begin{bmatrix} 1 \\ 0 \\ 0 \end{bmatrix} \Rightarrow spin(0^0), |1\rangle = \begin{bmatrix} 0 \\ 1 \\ 0 \end{bmatrix} \Rightarrow spin(120^0),$$

$$|2\rangle = \begin{bmatrix} 0 \\ 0 \\ 1 \end{bmatrix} \Rightarrow spin(240^0).$$

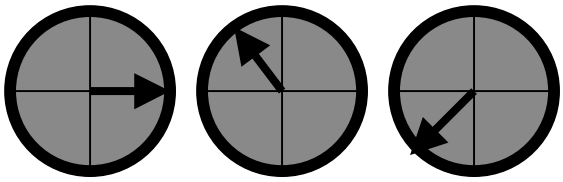

(a) (b) (c)

Figure 3. (a) Atomic particle spin of "0" degrees that represents qubit |0>, (b) atomic particle spin of "120" degrees that represents qubit |1>, and (c) atomic particle spin of "240" degrees that represents qubit |2>. A ternary m-qubit quantum register consists of m of such particle spins, thus can have up to 3^m distinct states.

In ternary logic, an n-qubit ternary quantum register is a vector of n ternary qubits. For a ternary quantum register composed of 2 ternary qubits, one obtains $3^2 = 9$ possible states of the ternary quantum register. These states are generated as follows:

$$|00\rangle = |0\rangle \otimes |0\rangle = \begin{bmatrix}1\\0\\0\end{bmatrix} \otimes \begin{bmatrix}1\\0\\0\end{bmatrix} = [1\ 0\ 0\ 0\ 0\ 0\ 0\ 0\ 0]^T,$$

$$|01\rangle = |0\rangle \otimes |1\rangle = \begin{bmatrix}1\\0\\0\end{bmatrix} \otimes \begin{bmatrix}0\\1\\0\end{bmatrix} = [0\ 1\ 0\ 0\ 0\ 0\ 0\ 0\ 0]^T,$$

$$|02\rangle = |0\rangle \otimes |2\rangle = \begin{bmatrix}1\\0\\0\end{bmatrix} \otimes \begin{bmatrix}0\\0\\1\end{bmatrix} = [0\ 0\ 1\ 0\ 0\ 0\ 0\ 0\ 0]^T,$$

$$|10\rangle = |1\rangle \otimes |0\rangle = \begin{bmatrix}0\\1\\0\end{bmatrix} \otimes \begin{bmatrix}1\\0\\0\end{bmatrix} = [0\ 0\ 0\ 1\ 0\ 0\ 0\ 0\ 0]^T,$$

$$|11\rangle = |1\rangle \otimes |1\rangle = \begin{bmatrix}0\\1\\0\end{bmatrix} \otimes \begin{bmatrix}0\\1\\0\end{bmatrix} = [0\ 0\ 0\ 0\ 1\ 0\ 0\ 0\ 0]^T,$$

$$|12\rangle = |1\rangle \otimes |2\rangle = \begin{bmatrix}0\\1\\0\end{bmatrix} \otimes \begin{bmatrix}0\\0\\1\end{bmatrix} = [0\ 0\ 0\ 0\ 0\ 1\ 0\ 0\ 0]^T,$$

$$|20\rangle = |2\rangle \otimes |0\rangle = \begin{bmatrix}0\\0\\1\end{bmatrix} \otimes \begin{bmatrix}1\\0\\0\end{bmatrix} = [0\ 0\ 0\ 0\ 0\ 0\ 1\ 0\ 0]^T,$$

$$|21\rangle = |2\rangle \otimes |1\rangle = \begin{bmatrix}0\\0\\1\end{bmatrix} \otimes \begin{bmatrix}0\\1\\0\end{bmatrix} = [0\ 0\ 0\ 0\ 0\ 0\ 0\ 1\ 0]^T,$$

$$|22\rangle = |2\rangle \otimes |2\rangle = \begin{bmatrix}0\\0\\1\end{bmatrix} \otimes \begin{bmatrix}0\\0\\1\end{bmatrix} = [0\ 0\ 0\ 0\ 0\ 0\ 0\ 0\ 1]^T \cdot$$

Where ⊗ is the tensor (Kronecker) product. In general, a ternary quantum register that is composed of k ternary qubits can have up to 3^k possible states. The ternary quantum register can be in any of the individual states at any instant of time or at all of the states at the same time. Due to the fact that multiple-valued quantum register can be at all of the states at the same time is the major reason of the multiple-valued parallelism that exists at the quantum level. For a quantum register composed of 1-ternary qubit, the evolution state $|\Psi\rangle$ is represented in terms of the computational basis states as follows:

$$|\Psi\rangle_{ternary-qubit} = \alpha|0\rangle + \beta|1\rangle + \gamma|2\rangle \qquad \textbf{(5)}$$

Where

$p(|0\rangle) = p_0 = \alpha\alpha^* = |\alpha|^2$, $p(|1\rangle) = p_1 = \beta\beta^* = |\beta|^2$,

$p(|2\rangle) = p_2 = \gamma\gamma^* = |\gamma|^2$,

* is the complex conjugate, $1 \geq p_i \geq 0$, $i \in \{0,1,2\}$, and $p_0 + p_1 + p_2 = 1$.

The meaning of the probability density p_i for ternary quantum logic is that p_0 is the probability of the quantum system being in state |0>, p_1 is the probability of the quantum system being in state |1>, and p_2 is the probability of the quantum system being in state |2>. Equation (5) can be written as:

$$|\Psi\rangle_{ternary-qubit} = \begin{bmatrix}|0\rangle & |1\rangle & |2\rangle\end{bmatrix} [E] \begin{bmatrix}\alpha\\\beta\\\gamma\end{bmatrix} \qquad \textbf{(6)}$$

Where [E] is the evolution matrix. For a 2-qubit ternary quantum register, one obtains:

$$|\Psi\rangle_{ternary-qubit1} = \alpha_1|0\rangle + \beta_1|1\rangle + \gamma_1|2\rangle$$

$$|\Psi\rangle_{ternary-qubit2} = \alpha_2|0\rangle + \beta_2|1\rangle + \gamma_2|2\rangle$$

$$|\Psi\rangle_{2-ternary-qubits} = |\Psi\rangle_1 \otimes |\Psi\rangle_2$$

$$= (\alpha_1|0\rangle + \beta_1|1\rangle + \gamma_1|2\rangle) \otimes (\alpha_2|0\rangle + \beta_2|1\rangle + \gamma_2|2\rangle)$$

$$= \alpha_1\alpha_2|00\rangle + \alpha_1\beta_2|01\rangle + \alpha_1\gamma_2|02\rangle + \beta_1\alpha_2|10\rangle + \beta_1\beta_2|11\rangle + \beta_1\gamma_2|12\rangle + \gamma_1\alpha_2|20\rangle + \gamma_1\beta_2|21\rangle + \gamma_1\gamma_2|22\rangle$$

$$\therefore |\Psi\rangle_{2-ternary-qubits} = \begin{bmatrix}|00\rangle\\|01\rangle\\|02\rangle\\|10\rangle\\|11\rangle\\|12\rangle\\|20\rangle\\|21\rangle\\|22\rangle\end{bmatrix}^T [E] \begin{bmatrix}\alpha_1\alpha_2\\\alpha_1\beta_2\\\alpha_1\gamma_2\\\beta_1\alpha_2\\\beta_1\beta_2\\\beta_1\gamma_2\\\gamma_1\alpha_2\\\gamma_1\beta_2\\\gamma_1\gamma_2\end{bmatrix} \qquad \textbf{(7)}$$

Where [E] is the quantum evolution matrix. For an N-ary quantum logic system the definition of quantum entanglement for multiple-valued quantum logic is a straightforward extension of equation (4). As the entanglement in the case of two-valued quantum systems seems to be the major factor behind the speedups of quantum

computations by which many computations are performed in parallel, the same role of entanglement is expected to be observed in the case of multiple-valued quantum systems. In this aspect, entanglement will be a special new resource in multiple-valued quantum computing. The following example illustrates the concept of multiple-valued quantum entanglement.

Example 1. (a) Consider a ternary quantum system of two qubits, given as:

$$\frac{1}{3}\left(|00\rangle+|01\rangle+|02\rangle+|10\rangle+|11\rangle+|12\rangle+|20\rangle+|21\rangle+|22\rangle\right)$$
$$=\frac{1}{\sqrt{3}}\left(|0\rangle+|1\rangle+|2\rangle\right)\otimes\frac{1}{\sqrt{3}}\left(|0\rangle+|1\rangle+|2\rangle\right)$$
$$=\frac{1}{\sqrt{3}}\left(|0\rangle+|1\rangle+|2\rangle\right)\frac{1}{\sqrt{3}}\left(|0\rangle+|1\rangle+|2\rangle\right)$$

This system is decomposable, as the functions of the first and second qubits are disentangled according to equation (4).

(b) Consider now the ternary quantum system:

$$\frac{1}{\sqrt{3}}\left(|02\rangle+|10\rangle\right)$$

This system is entangled, as no decomposition according to equation (4) is possible.

The following theorems present the ternary quantum "composite" basis states and the ternary quantum Einstein-Podolsky-Rosen (EPR) basis states, respectively [2]. Such basis states serve in the construction of the corresponding canonical representations of multiple-valued quantum circuits, like multiple-valued quantum evolution decision trees and diagrams (that will be presented in subsection 3.2). Such new multiple-valued representations are important because the new forms of quantum decision trees and diagrams, that are produced using multiple-valued EPR basis states, allow for further possible optimizations in the design of the corresponding quantum circuits. This is analogous to the classical case where various representations of logic circuits lead to different scales of optimizations (area, speed, etc) in the synthesis of the corresponding logic circuits [18]. Although the results that are presented in the following sections are for the ternary case, generalization to higher radices is straightforward.

Theorem 1. The following represents the ternary "composite" basis states:

$$\{\ |+\rangle=\frac{|0\rangle+d_1|1\rangle+d_2|2\rangle}{\sqrt{3}},|\|\rangle=\frac{|0\rangle+|1\rangle+|2\rangle}{\sqrt{3}},$$
$$|-\rangle=\frac{|0\rangle+d_2|1\rangle+d_1|2\rangle}{\sqrt{3}}\ \}$$
$$Where:|0\rangle=\frac{|+\rangle+|\|\rangle+|-\rangle}{\sqrt{3}},|1\rangle=\frac{d_2|+\rangle+|\|\rangle+d_1|-\rangle}{\sqrt{3}},$$
$$|2\rangle=\frac{d_1|+\rangle+|\|\rangle+d_2|-\rangle}{\sqrt{3}},d_2=-(1+d_1)=-\frac{1}{2}(1+\sqrt{3}i)=e^{\frac{4\pi i}{3}},$$
$$d_1=-(1+d_2)=-\frac{1}{2}(1-\sqrt{3}i)=e^{\frac{2\pi i}{3}}.$$

Proof. We utilize the orthogonal ternary Chrestenson spectral transform [14] for a single variable:

$$C_{(1)}^{(3)}=\begin{bmatrix}1 & 1 & 1\\ 1 & d_1 & d_2\\ 1 & d_2 & d_1\end{bmatrix}$$

Due to the fact that the evolution process must be unitary, one obtains the following normalized Chrestenson spectral transform:

$$C_{(1)\ normalized}^{(3)}=\frac{1}{\sqrt{3}}\begin{bmatrix}1 & 1 & 1\\ 1 & d_1 & d_2\\ 1 & d_2 & d_1\end{bmatrix}$$

By using the normalized Chrestenson transformation as the evolution matrix, one obtains the corresponding output composite basis states in Theorem 1, for the corresponding ternary input $|\Psi\rangle=\alpha|0\rangle+\beta|1\rangle+\gamma|2\rangle$. **Q.E.D.**

Theorem 2. For the following ternary inputs:

$$|00\rangle,|01\rangle,|02\rangle,|10\rangle,|11\rangle,|12\rangle,|20\rangle,|21\rangle,|22\rangle$$

The following represents the set of ternary 2-qubit orthonormal Einstein-Podolsky-Rosen (EPR) basis states, respectively:

$$\frac{|00\rangle+|11\rangle+|22\rangle}{\sqrt{3}},\frac{|01\rangle+|12\rangle+|20\rangle}{\sqrt{3}},\frac{|02\rangle+|10\rangle+|21\rangle}{\sqrt{3}},$$
$$\frac{|00\rangle+d_1|11\rangle+d_2|22\rangle}{\sqrt{3}},\frac{|01\rangle+d_1|12\rangle+d_2|20\rangle}{\sqrt{3}},\frac{|02\rangle+d_1|10\rangle+d_2|21\rangle}{\sqrt{3}},$$
$$\frac{|00\rangle+d_2|11\rangle+d_1|22\rangle}{\sqrt{3}},\frac{|01\rangle+d_2|12\rangle+d_1|20\rangle}{\sqrt{3}},\frac{|02\rangle+d_2|10\rangle+d_1|21\rangle}{\sqrt{3}}$$

Where:

$d_2=-(1+d_1)=-\frac{1}{2}(1+\sqrt{3}i)=e^{\frac{4\pi i}{3}}$, $d_1=-(1+d_2)=$
$-\frac{1}{2}(1-\sqrt{3}i)=e^{\frac{2\pi i}{3}}$.

Full proof of Theorem 2 is given in [2].

Example 2. The following is the derivation of the probability amplitudes of the ternary composite basis states that are presented in Theorem 1. By using the ternary quantum signal $|\Psi\rangle = \alpha|0\rangle + \beta|1\rangle + \gamma|2\rangle$ as an input to the ternary quantum Chrestenson gate: $C^{(3)}_{(1)\,normalized} = \frac{1}{\sqrt{3}}\begin{bmatrix} 1 & 1 & 1 \\ 1 & d_1 & d_2 \\ 1 & d_2 & d_1 \end{bmatrix}$, one obtains the following quantum signal at the output of the quantum Chrestenson gate:

$$|\Psi\rangle' = [|0\rangle \quad |1\rangle \quad |2\rangle]\frac{1}{\sqrt{3}}\begin{bmatrix} 1 & 1 & 1 \\ 1 & d_1 & d_2 \\ 1 & d_2 & d_1 \end{bmatrix}\begin{bmatrix} \alpha \\ \beta \\ \gamma \end{bmatrix}$$

$$= [|0\rangle \quad |1\rangle \quad |2\rangle]\begin{bmatrix} \frac{\alpha+\beta+\gamma}{\sqrt{3}} \\ \frac{\alpha+d_1\beta+d_2\gamma}{\sqrt{3}} \\ \frac{\alpha+d_2\beta+d_1\gamma}{\sqrt{3}} \end{bmatrix}$$

$$= \frac{\alpha+\beta+\gamma}{\sqrt{3}}|0\rangle + \frac{\alpha+d_1\beta+d_2\gamma}{\sqrt{3}}|1\rangle + \frac{\alpha+d_2\beta+d_1\gamma}{\sqrt{3}}|2\rangle$$

$$|\Psi\rangle' = [|0\rangle \quad |1\rangle \quad |2\rangle]\frac{1}{\sqrt{3}}\begin{bmatrix} 1 & 1 & 1 \\ 1 & d_1 & d_2 \\ 1 & d_2 & d_1 \end{bmatrix}\begin{bmatrix} \alpha \\ \beta \\ \gamma \end{bmatrix}$$

$$= \begin{bmatrix} \frac{|0\rangle+|1\rangle+|2\rangle}{\sqrt{3}} & \frac{|0\rangle+d_1|1\rangle+d_2|2\rangle}{\sqrt{3}} & \frac{|0\rangle+d_2|1\rangle+d_1|2\rangle}{\sqrt{3}} \end{bmatrix}\begin{bmatrix} \alpha \\ \beta \\ \gamma \end{bmatrix}$$

$$= [|\|\rangle \quad |+\rangle \quad |-\rangle]\begin{bmatrix} \alpha \\ \beta \\ \gamma \end{bmatrix} = \alpha|\|\rangle + \beta|+\rangle + \gamma|-\rangle$$

Where:

$$\{\,|+\rangle = \frac{|0\rangle+d_1|1\rangle+d_2|2\rangle}{\sqrt{3}}, |\|\rangle = \frac{|0\rangle+|1\rangle+|2\rangle}{\sqrt{3}},$$

$$|-\rangle = \frac{|0\rangle+d_2|1\rangle+d_1|2\rangle}{\sqrt{3}}\ \},$$

$$\{|0\rangle = \frac{|+\rangle+|\|\rangle+|-\rangle}{\sqrt{3}}, |1\rangle = \frac{d_2|+\rangle+|\|\rangle+d_1|-\rangle}{\sqrt{3}},$$

$$|2\rangle = \frac{d_1|+\rangle+|\|\rangle+d_2|-\rangle}{\sqrt{3}}\}.$$

Consequently, one obtains at the input side of the quantum Chrestenson gate the following quantum state:

$$\therefore |\Psi\rangle = \alpha|0\rangle + \beta|1\rangle + \gamma|2\rangle = \alpha\frac{|+\rangle+|\|\rangle+|-\rangle}{\sqrt{3}} + \beta\frac{d_2|+\rangle+|\|\rangle+d_1|-\rangle}{\sqrt{3}} + \gamma\frac{d_1|+\rangle+|\|\rangle+d_2|-\rangle}{\sqrt{3}}$$

$$= \frac{\alpha+d_2\beta+d_1\gamma}{\sqrt{3}}|+\rangle + \frac{\alpha+\beta+\gamma}{\sqrt{3}}|\|\rangle + \frac{\alpha+d_1\beta+d_2\gamma}{\sqrt{3}}|-\rangle$$

Therefore, one obtains the following probability amplitudes:

$$\sqrt{p_{|\|\rangle}} = \frac{|\alpha+\beta+\gamma|}{\sqrt{3}}, \quad \sqrt{p_{|-\rangle}} = \frac{|\alpha+d_1\beta+d_2\gamma|}{\sqrt{3}},$$

and $\sqrt{p_{|+\rangle}} = \frac{|\alpha+d_2\beta+d_1\gamma|}{\sqrt{3}}$

Consequently, measuring $|\Psi\rangle$ with respect to the new basis $\{|\|\rangle, |+\rangle, |-\rangle\}$ will result into the state $|\|\rangle$ with probability $\frac{|\alpha+\beta+\gamma|^2}{3}$, will result into the state $|-\rangle$ with probability $\frac{|\alpha+d_1\beta+d_2\gamma|^2}{3}$, and will result into the state $|+\rangle$ with probability $\frac{|\alpha+d_2\beta+d_1\gamma|^2}{3}$, respectively.

Figure 4 shows factorizations of serially interconnected evolution processes that resemble equivalencies between ternary quantum logic circuits, using the ternary quantum Chrestenson operator $C^{(3)}_{(1)\,normalized} = \frac{1}{\sqrt{3}}\begin{bmatrix} 1 & 1 & 1 \\ 1 & d_1 & d_2 \\ 1 & d_2 & d_1 \end{bmatrix}$, which was presented in Theorem 1. More quantum equivalencies are shown in [2]. The equivalencies of the serially interconnected quantum Chrestenson primitives can be utilized in the synthesis of quantum logic circuits by replacing long serial gate interconnections with their equivalent circuits (i.e., technology mapping). For instance, such transformations can be applied to a quantum logic circuit that is created by a genetic algorithm (GA) or other evolutionary algorithms [19].

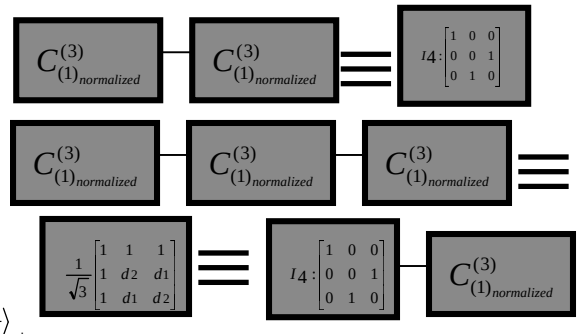

Figure 4. Multiple-valued quantum logic circuit equivalence using quantum Chrestenson gate.

3.2. New Multiple-Valued Quantum Gates, Evolution Processes, and Canonical Representations

The following presents ternary logic evolution processes over GF(3) for the ternary Feynman, and Swap quantum gates, respectively. The input qubit to the ternary quantum gate is the column index of the ternary evolution matrix, and the output qubit of the ternary quantum gate is the row index of the ternary evolution matrix. The column and row indices of the ternary evolution matrix take the following order for (1,1), (2,2), and (3,3) quantum gates, respectively:

$\Rightarrow 1input-1output \quad gate: |0\rangle,|1\rangle,|2\rangle$

$\Rightarrow 2input-2output \quad gate: |00\rangle,|01\rangle,|02\rangle,|10\rangle,|11\rangle,|12\rangle,|20\rangle, |21\rangle,|22\rangle$

$\Rightarrow 3input-3output \quad gate: |000\rangle,|001\rangle,|002\rangle,|010\rangle,|011\rangle,|012\rangle, |020\rangle,|021\rangle,|022\rangle,|100\rangle,|101\rangle,|102\rangle,|110\rangle,|111\rangle,|112\rangle,|120\rangle,|121\rangle, |122\rangle,|200\rangle,|201\rangle,|202\rangle,|210\rangle,|211\rangle,|212\rangle,|220\rangle,|221\rangle,|222\rangle$

The following multiple-valued evolution matrices will be useful in the synthesis of multiple-valued quantum circuits. For instance, by using evolutionary algorithms for the synthesis of minimal size multiple-valued quantum circuits [19], one can consider the fitness function of the evolutionary algorithms (such as genetic programming or genetic algorithms) to contain two components: one component is for the correctness of the resulting function (e.g., error is zero), and the other component is for the cost of the resulting quantum circuit (e.g., number of gates). The synthesis of such multiple-valued quantum circuits, using evolutionary algorithms, is done through the calculation of the final evolution matrix of the whole circuit by using normal matrix multiplication (serial logic interconnects) and tensor multiplication (parallel logic interconnects) of the individual evolution matrices (gates). Example 3 will illustrate such serial, and parallel algebraic manipulations for the analysis of the corresponding multiple-valued quantum logic circuits.

Theorem 3. The following is the ternary Galois-field Feynman evolution matrix:

$$Feynman = \begin{bmatrix} 1&0&0&0&0&0&0&0&0 \\ 0&1&0&0&0&0&0&0&0 \\ 0&0&1&0&0&0&0&0&0 \\ 0&0&0&0&0&1&0&0&0 \\ 0&0&0&1&0&0&0&0&0 \\ 0&0&0&0&1&0&0&0&0 \\ 0&0&0&0&0&0&0&1&0 \\ 0&0&0&0&0&0&0&0&1 \\ 0&0&0&0&0&0&1&0&0 \end{bmatrix}$$

Proof. Utilizing the algebraic addition and multiplication operations over Galois-field (from Figure 2), one obtains the following *quantum transformations* of the ternary input qubits into the output qubits using GF(3) Feynman quantum register:

$|00\rangle \rightarrow |00\rangle,|01\rangle \rightarrow |01\rangle,|02\rangle \rightarrow |02\rangle,|10\rangle \rightarrow |11\rangle,|11\rangle \rightarrow |12\rangle$

$|12\rangle \rightarrow |10\rangle,|20\rangle \rightarrow |22\rangle,|21\rangle \rightarrow |20\rangle,|22\rangle \rightarrow |21\rangle$

Then by solving for the following set of linearly independent equations over ternary Galois-field:

$$\begin{bmatrix} \alpha1&\alpha2&\alpha3&\alpha4&\alpha5&\alpha6&\alpha7&\alpha8&\alpha9 \\ \beta1&\beta2&\beta3&\beta4&\beta5&\beta6&\beta7&\beta8&\beta9 \\ \chi1&\chi2&\chi3&\chi4&\chi5&\chi6&\chi7&\chi8&\chi9 \\ \delta1&\delta2&\delta3&\delta4&\delta5&\delta6&\delta7&\delta8&\delta9 \\ \varepsilon1&\varepsilon2&\varepsilon3&\varepsilon4&\varepsilon5&\varepsilon6&\varepsilon7&\varepsilon8&\varepsilon9 \\ \phi1&\phi2&\phi3&\phi4&\phi5&\phi6&\phi7&\phi8&\phi9 \\ \varphi1&\varphi2&\varphi3&\varphi4&\varphi5&\varphi6&\varphi7&\varphi8&\varphi9 \\ \gamma1&\gamma2&\gamma3&\gamma4&\gamma5&\gamma6&\gamma7&\gamma8&\gamma9 \\ \eta1&\eta2&\eta3&\eta4&\eta5&\eta6&\eta7&\eta8&\eta9 \end{bmatrix} |00\rangle = |00\rangle$$

$$\bullet\bullet\bullet$$

$$\begin{bmatrix} \alpha1&\alpha2&\alpha3&\alpha4&\alpha5&\alpha6&\alpha7&\alpha8&\alpha9 \\ \beta1&\beta2&\beta3&\beta4&\beta5&\beta6&\beta7&\beta8&\beta9 \\ \chi1&\chi2&\chi3&\chi4&\chi5&\chi6&\chi7&\chi8&\chi9 \\ \delta1&\delta2&\delta3&\delta4&\delta5&\delta6&\delta7&\delta8&\delta9 \\ \varepsilon1&\varepsilon2&\varepsilon3&\varepsilon4&\varepsilon5&\varepsilon6&\varepsilon7&\varepsilon8&\varepsilon9 \\ \phi1&\phi2&\phi3&\phi4&\phi5&\phi6&\phi7&\phi8&\phi9 \\ \varphi1&\varphi2&\varphi3&\varphi4&\varphi5&\varphi6&\varphi7&\varphi8&\varphi9 \\ \gamma1&\gamma2&\gamma3&\gamma4&\gamma5&\gamma6&\gamma7&\gamma8&\gamma9 \\ \eta1&\eta2&\eta3&\eta4&\eta5&\eta6&\eta7&\eta8&\eta9 \end{bmatrix} |22\rangle = |21\rangle$$

One obtains the GF(3) Feynman evolution matrix shown in Theorem 3. **Q.E.D.**

Theorem 4. The following is the ternary Galois-field Swap evolution matrix:

$$Swap = \begin{bmatrix} 1&0&0&0&0&0&0&0&0 \\ 0&0&0&1&0&0&0&0&0 \\ 0&0&0&0&0&0&1&0&0 \\ 0&1&0&0&0&0&0&0&0 \\ 0&0&0&0&1&0&0&0&0 \\ 0&0&0&0&0&0&0&1&0 \\ 0&0&1&0&0&0&0&0&0 \\ 0&0&0&0&0&1&0&0&0 \\ 0&0&0&0&0&0&0&0&1 \end{bmatrix}$$

Proof. Utilizing the algebraic addition and multiplication operations over Galois-Field (from Figure 2), one obtains the following *quantum transformations* of the ternary input qubits into the output qubits using the ternary Swap quantum register:

$|00\rangle \rightarrow |00\rangle,|01\rangle \rightarrow |10\rangle,|02\rangle \rightarrow |20\rangle,|10\rangle \rightarrow |01\rangle,|11\rangle \rightarrow |11\rangle$

$|12\rangle \rightarrow |21\rangle,|20\rangle \rightarrow |02\rangle,|21\rangle \rightarrow |12\rangle,|22\rangle \rightarrow |22\rangle$

Similar to Theorem 3, by solving for the set of linearly independent equations over ternary Galois-field, one obtains the ternary Swap Galois-field evolution matrix. **Q.E.D.**

Example 3. The following circuit represents a mixture of serial and parallel-like interconnects between multiple-valued quantum primitives.

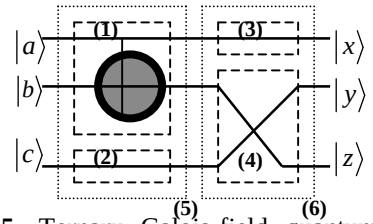

Figure 5. Ternary Galois-field quantum circuit composed of serial interconnect of two parallel ternary Galois-field circuits: dashed boxes ((1),(2) and (3),(4)) in each sub-circuit are parallel connected, and dotted boxes (5) and (6) are serially interconnected.

Let us evolve the input qubit |122> using the multiple-valued quantum circuit in Figure 5. This is done using the following two quantum synthesis rules: (1) the total multiple-valued quantum evolution transformation $[M]$ of the total serially interconnected quantum circuit is equal to the normal matrix multiplication of the individual evolution matrices $[N_q]$ that correspond to the individual quantum primitives, i.e. $[M]_{serial} = \prod_q [N_q]$, and (2) the total evolution transformation $[M]$ of the total parallel-interconnected quantum circuit is equal to the tensor (Kronecker) product of the individual evolution matrices $[N_q]$ that correspond to the individual quantum primitives, i.e. $[M]_{parallel} = \otimes [N]_q$. The evolution of the input ternary qubit, in Figure 5, can be viewed in two equivalent perspectives, respectively. One perspective is to evolve the input qubit stage by stage. The second perspective is to evolve the input qubit using the total quantum circuit at once. The evolution matrices of the parallel-connected dashed boxes in (5) and (6), are as follows, respectively (Where the symbol || means parallel connection):

$\Rightarrow$ (5) = (1) || (2): Feynman $\otimes$ Wire =

$$\begin{bmatrix} 1&0&0&0&0&0&0&0&0\\ 0&1&0&0&0&0&0&0&0\\ 0&0&1&0&0&0&0&0&0\\ 0&0&0&0&0&1&0&0&0\\ 0&0&0&1&0&0&0&0&0\\ 0&0&0&0&1&0&0&0&0\\ 0&0&0&0&0&0&0&1&0\\ 0&0&0&0&0&0&0&0&1\\ 0&0&0&0&0&0&1&0&0 \end{bmatrix} \otimes \begin{bmatrix} 1&0&0\\ 0&1&0\\ 0&0&1 \end{bmatrix} =$$

$$\begin{bmatrix} \begin{bmatrix} 1&0&0\\ 0&1&0\\ 0&0&1 \end{bmatrix} & & & & & & & & \\ & \begin{bmatrix} 1&0&0\\ 0&1&0\\ 0&0&1 \end{bmatrix} & & & & & & & \\ & & \begin{bmatrix} 1&0&0\\ 0&1&0\\ 0&0&1 \end{bmatrix} & & & & & & \\ & & & \begin{bmatrix} 1&0&0\\ 0&1&0\\ 0&0&1 \end{bmatrix} & & & & & \\ & & & & \begin{bmatrix} 1&0&0\\ 0&1&0\\ 0&0&1 \end{bmatrix} & & & & \\ & & & & & \begin{bmatrix} 1&0&0\\ 0&1&0\\ 0&0&1 \end{bmatrix} & & & \\ & & & & & & \begin{bmatrix} 1&0&0\\ 0&1&0\\ 0&0&1 \end{bmatrix} & & \\ & & & & & & & \begin{bmatrix} 1&0&0\\ 0&1&0\\ 0&0&1 \end{bmatrix} & \\ & & & & & & & & \begin{bmatrix} 1&0&0\\ 0&1&0\\ 0&0&1 \end{bmatrix} \end{bmatrix}$$

$\Rightarrow$ (6) = (3) || (4): Wire $\otimes$ Swap =

$$\begin{bmatrix} 1&0&0\\ 0&1&0\\ 0&0&1 \end{bmatrix} \otimes \begin{bmatrix} 1&0&0&0&0&0&0&0&0\\ 0&0&0&1&0&0&0&0&0\\ 0&0&0&0&0&0&0&1&0\\ 0&1&0&0&0&0&0&0&0\\ 0&0&0&0&1&0&0&0&0\\ 0&0&0&0&0&0&0&1&0\\ 0&0&1&0&0&0&0&0&0\\ 0&0&0&0&0&1&0&0&0\\ 0&0&0&0&0&0&0&0&1 \end{bmatrix} =$$

$$\begin{bmatrix} \begin{bmatrix} 1&0&0&0&0&0&0&0&0\\ 0&0&0&1&0&0&0&0&0\\ 0&0&0&0&0&0&0&1&0\\ 0&1&0&0&0&0&0&0&0\\ 0&0&0&0&1&0&0&0&0\\ 0&0&0&0&0&0&0&1&0\\ 0&0&1&0&0&0&0&0&0\\ 0&0&0&0&0&1&0&0&0\\ 0&0&0&0&0&0&0&0&1 \end{bmatrix} & & \\ & \begin{bmatrix} 1&0&0&0&0&0&0&0&0\\ 0&0&0&1&0&0&0&0&0\\ 0&0&0&0&0&0&0&1&0\\ 0&1&0&0&0&0&0&0&0\\ 0&0&0&0&1&0&0&0&0\\ 0&0&0&0&0&0&0&1&0\\ 0&0&1&0&0&0&0&0&0\\ 0&0&0&0&0&1&0&0&0\\ 0&0&0&0&0&0&0&0&1 \end{bmatrix} & \\ & & \begin{bmatrix} 1&0&0&0&0&0&0&0&0\\ 0&0&0&1&0&0&0&0&0\\ 0&0&0&0&0&0&0&1&0\\ 0&1&0&0&0&0&0&0&0\\ 0&0&0&0&1&0&0&0&0\\ 0&0&0&0&0&0&0&1&0\\ 0&0&1&0&0&0&0&0&0\\ 0&0&0&0&0&1&0&0&0\\ 0&0&0&0&0&0&0&0&1 \end{bmatrix} \end{bmatrix}$$

$\Rightarrow$ input = input_1 = $|122\rangle$ = $|1\rangle \otimes |2\rangle \otimes |2\rangle$

Perspective #1: *$input_1 \Rightarrow$ (5) $\Rightarrow$ $output_1$, $output_1$ (= $input_2$) $\Rightarrow$ (6) $\Rightarrow$ $output_2$*

The quantum circuit that is shown in Figure 5 evolves the input qubit |122> into the output qubit |120>.

Perspective #2: *$input_1 \Rightarrow$ ((6)(5)) $\Rightarrow$ $output_2$*

The quantum circuit shown in Figure 5 evolves the qubit |122> into the qubit |120> (which is the same result that is obtained in perspective #1).

The following are new multiple-valued quantum permuters that can be used in the future synthesis of multiple-valued quantum logic circuits, where ± 1 and $\pm i$ means that any combination of positive and negative 1 and any combination of positive and negative *i* can occur, respectively.

Pauli-X:

$$I_0:\begin{bmatrix}0&0&1\\0&1&0\\1&0&0\end{bmatrix}, I_1:\begin{bmatrix}0&1&0\\1&0&0\\0&0&1\end{bmatrix}, I_2:\begin{bmatrix}0&1&0\\0&0&1\\1&0&0\end{bmatrix},$$

$$I_3:\begin{bmatrix}0&0&1\\1&0&0\\0&1&0\end{bmatrix}, I_4:\begin{bmatrix}1&0&0\\0&0&1\\0&1&0\end{bmatrix}, I_5:\begin{bmatrix}1&0&0\\0&1&0\\0&0&1\end{bmatrix}$$

Pauli-Y:

$$I_6:\begin{bmatrix}0&0&\pm i\\0&\pm i&0\\\pm i&0&0\end{bmatrix}, I_7:\begin{bmatrix}0&\pm i&0\\\pm i&0&0\\0&0&\pm i\end{bmatrix}, I_8:\begin{bmatrix}0&\pm i&0\\0&0&\pm i\\\pm i&0&0\end{bmatrix},$$

$$I_9:\begin{bmatrix}0&0&\pm i\\\pm i&0&0\\0&\pm i&0\end{bmatrix}, I_{10}:\begin{bmatrix}\pm i&0&0\\0&0&\pm i\\0&\pm i&0\end{bmatrix}, I_{11}:\begin{bmatrix}\pm i&0&0\\0&\pm i&0\\0&0&\pm i\end{bmatrix}$$

More classes of the quantum permuters are shown in [2].

Utilizing Theorems 3 and 4, the following is the GF(3) quantum Buffer (which is equivalent to two wires), Feynman (Theorem 3), and Swap (Theorem 4) evolution processes, for the ternary computational basis states $\{|00\rangle,|01\rangle,|02\rangle,|10\rangle,|11\rangle,|12\rangle,|20\rangle,|21\rangle,|22\rangle\}$, respectively.

$$|\Psi\rangle_{Buffer} = \begin{bmatrix}|00\rangle\\|01\rangle\\|02\rangle\\|10\rangle\\|11\rangle\\|12\rangle\\|20\rangle\\|21\rangle\\|22\rangle\end{bmatrix}^T \begin{bmatrix}1&0&0&0&0&0&0&0&0\\0&1&0&0&0&0&0&0&0\\0&0&1&0&0&0&0&0&0\\0&0&0&1&0&0&0&0&0\\0&0&0&0&1&0&0&0&0\\0&0&0&0&0&1&0&0&0\\0&0&0&0&0&0&1&0&0\\0&0&0&0&0&0&0&1&0\\0&0&0&0&0&0&0&0&1\end{bmatrix} \begin{bmatrix}\alpha 1\alpha 2\\\alpha 1\beta 2\\\alpha 1\gamma 2\\\beta 1\alpha 2\\\beta 1\beta 2\\\beta 1\gamma 2\\\gamma 1\alpha 2\\\gamma 1\beta 2\\\gamma 1\gamma 2\end{bmatrix} \quad \textbf{(8)}$$

$$|\Psi\rangle_{Feynman} = \begin{bmatrix}|00\rangle\\|01\rangle\\|02\rangle\\|10\rangle\\|11\rangle\\|12\rangle\\|20\rangle\\|21\rangle\\|22\rangle\end{bmatrix}^T \begin{bmatrix}1&0&0&0&0&0&0&0&0\\0&1&0&0&0&0&0&0&0\\0&0&1&0&0&0&0&0&0\\0&0&0&0&0&1&0&0&0\\0&0&0&1&0&0&0&0&0\\0&0&0&0&1&0&0&0&0\\0&0&0&0&0&0&0&1&0\\0&0&0&0&0&0&0&0&1\\0&0&0&0&0&0&1&0&0\end{bmatrix} \begin{bmatrix}\alpha 1\alpha 2\\\alpha 1\beta 2\\\alpha 1\gamma 2\\\beta 1\alpha 2\\\beta 1\beta 2\\\beta 1\gamma 2\\\gamma 1\alpha 2\\\gamma 1\beta 2\\\gamma 1\gamma 2\end{bmatrix} \quad \textbf{(9)}$$

$$|\Psi\rangle_{Swap} = \begin{bmatrix}|00\rangle\\|01\rangle\\|02\rangle\\|10\rangle\\|11\rangle\\|12\rangle\\|20\rangle\\|21\rangle\\|22\rangle\end{bmatrix}^T \begin{bmatrix}1&0&0&0&0&0&0&0&0\\0&0&0&1&0&0&0&0&0\\0&0&0&0&0&0&1&0&0\\0&1&0&0&0&0&0&0&0\\0&0&0&0&1&0&0&0&0\\0&0&0&0&0&0&0&1&0\\0&0&1&0&0&0&0&0&0\\0&0&0&0&0&1&0&0&0\\0&0&0&0&0&0&0&0&1\end{bmatrix} \begin{bmatrix}\alpha 1\alpha 2\\\alpha 1\beta 2\\\alpha 1\gamma 2\\\beta 1\alpha 2\\\beta 1\beta 2\\\beta 1\gamma 2\\\gamma 1\alpha 2\\\gamma 1\beta 2\\\gamma 1\gamma 2\end{bmatrix} \quad \textbf{(10)}$$

Since various types of decision trees and diagrams are of fundamental importance in binary, multiple-valued, Reed-Muller, Galois-field, arithmetic, and fuzzy logics [6,18], it is obvious that they will be also useful in binary quantum logic which is a generalization of binary logic, and in multiple-valued quantum logic which is a generalization of multiple-valued logic, where the concepts of quantum decision trees and diagrams have not been introduced so far in the known literature. Figure 6 represents the corresponding ternary Buffer (equation (8)), Feynman (equation (9)), and Swap (equation (10)) multiple-valued quantum evolution decision trees (**MvQEDTs**) for the ternary computational basis states, $\{|00\rangle,|01\rangle,|02\rangle,|10\rangle,|11\rangle,|12\rangle,|20\rangle,|21\rangle,|22\rangle\}$, respectively. The new quantum evolution decision tree representation can be useful in the future algorithms for the synthesis of quantum logic circuits, analogous to the already existing algorithms that depend on such representation for the optimized synthesis of classical (non-quantum) logic circuits [18].

The ternary quantum decision trees in Figures 6a and 6b can be computed for the ternary composite basis states $\{|\,|\rangle,|\,|+\rangle,|\,|-\rangle,|+|\rangle|++\rangle|+-\rangle|-|\rangle|-+\rangle|--\rangle\}$ (that were produced in Theorem 1 and Example 2), for which the states $|00\rangle,|01\rangle,|02\rangle,|10\rangle,|11\rangle,|12\rangle,|20\rangle,|21\rangle,|22\rangle$ are replaced by the states $\{|\,|\rangle,|\,|+\rangle,|\,|-\rangle,|+|\rangle|++\rangle|+-\rangle|-|\rangle|-+\rangle|--\rangle\}$, respectively. Although the values in the leafs of the MvQEDT in Figures 6a and 6b are not equal to each other in general, multiple-valued quantum evolution decision diagrams (**MvQEDDs**) can be constructed for the corresponding multiple-valued quantum evolution decision trees. The rules for such quantum decision diagrams are the same as in classical decision diagrams: (1) join isomorphic nodes, and (2) remove redundant nodes [6,18]. Figure 6c illustrates one case for the concept of ternary quantum evolution decision diagrams.

One notes that for specific order of variables, the resulting MvQEDTs (Figures 6a and 6b) and MvQEDDs (Figure 6c) are canonical. Obviously, from the software implementation point of view, and similar to the tools for classical multiple-valued and fuzzy logics [18], quantum decision diagrams (Figure 6c) can be realized on top of standard binary decision diagram (BDD) packages.

4. Conclusion

Multiple-valued Einstein-Podolsky-Rosen (EPR) basis states have been presented. The new multiple-valued EPR basis states serve in the construction of the corresponding canonical representations of multiple-valued quantum circuits, like multiple-valued quantum evolution decision trees and diagrams. Such new multiple-valued representations are important because the new forms of quantum decision trees and diagrams, that are produced using multiple-valued EPR basis states, can allow for further possible optimizations in the design of quantum circuits, analogous to the classical (non-quantum) cases [18]. The new multiple-valued quantum EPR basis states have been achieved by utilizing the quantum Chrestenson operator, which is also presented in this work. New Galois-field multiple-valued quantum gates, evolution processes, and the corresponding canonical quantum decision trees and decision diagrams were also introduced as a first attempt of developing multiple-valued quantum logic elements, representations, and synthesis methods. Future work will involve the investigation of other canonical and regular structures for the realization of arbitrary quantum logic circuits such as quantum lattice structures [2] and quantum butterfly diagrams [2]. Also the investigation of using the entanglement in speeding up multiple-valued quantum computations will be conducted.

5. References

[1] A. Al-Rabadi, "On the Characterization of Multi-Valued Equally Input-Output Reversible Galois Logic Primitives", *Technical Report #2001/006*, ECE Department, Portland State University, Portland, Oregon, 1st August 2001.

[2] A. Al-Rabadi, "Synthesis and Canonical Representations of Equally Input-Output Binary and Multiple-Valued Galois Quantum Logic: Decision Trees, Decision Diagrams, Quantum Butterflies, Quantum Chrestenson Gate, and Multiple-Valued Bell-Einstein-Podolsky-Rosen Basis States", *Technical Report #2001/007*, ECE Department, Portland State University, Portland, Oregon, 22nd August 2001.

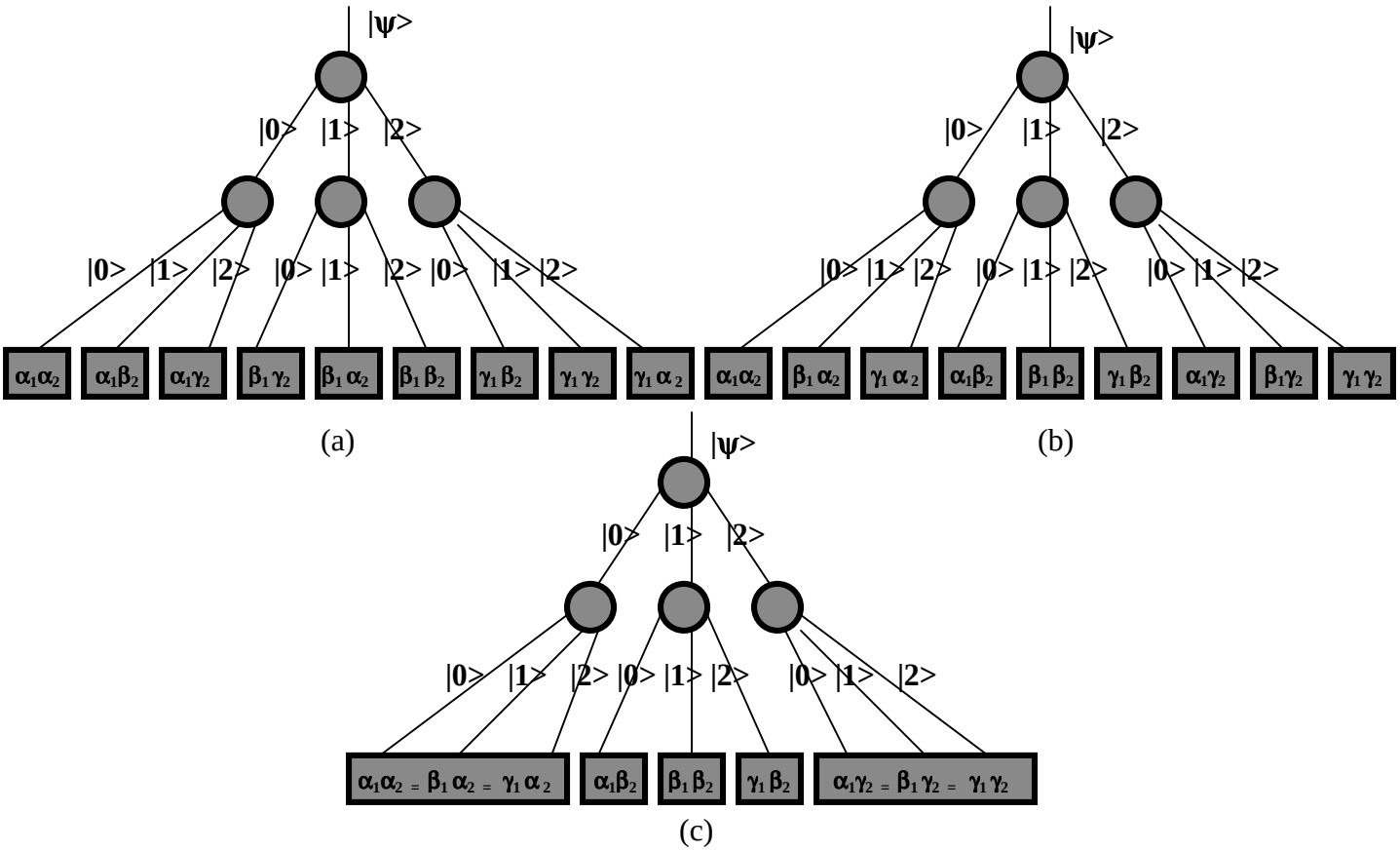

Figure 6. Ternary quantum evolution decision trees: (a) Feynman, (b) Swap, and (c) Swap evolution decision diagram (QDD) for the ternary computational basis states, where $\{\alpha_i, \beta_j, \gamma_k\}$ are the probability amplitudes.

[3] A. Al-Rabadi, "New Reversible Invariant Multi-Valued Families of Spectral Transforms For Three-Dimensional Layout", *Technical Report #2001/003*, ECE Department, Portland State University, Portland, Oregon, 3rd March 2001.

[4] A. Al-Rabadi, and M. Perkowski, "New Classes of Multi-Valued Reversible Decompositions for Three-Dimensional Layout" *Proc. Reed-Muller'2001*, pp 185-204, Starkville, Mississippi, 2001.

[5] C. Bennett, "Logical Reversibility of computation". *IBM Journal of Research and Development*, 17, pp.525-532, 1973.

[6] R. E. Bryant," Graph-based algorithms for Boolean functions manipulation," *IEEE Trans. On Comp.*, Vol. C-35, No.8, pp. 667-691, 1986.

[7] A. Calderbank, E. Rains, P. Shor, and N. Sloane, "Quantum Error Correction Via Codes Over GF(4)", *AT&T Labs-Research*, 5th March 1998.

[8] I. Chuang, and Y. Yamamoto, "A Simple Quantum Computer", *ERATO Quantum Fluctuation Project*, Edward L. Ginzton Laboratory, Stanford University, 28 March 1995.

[9] P. A. M. Dirac, *The Principles of Quantum Mechanics*, first edition, Oxford University Press, 1930.

[10] R. Feynman, *Feynman Lectures On Computation*, Addison Wesley, 1996.

[11] E. Fredkin and T. Toffoli, "Conservative Logic", *Int. Journal of Theoretical Physics*, **21**, pp.219-253, 1982.

[12] P. Kerntopf, "A Comparison of Logical Efficiency of Reversible and Conventional Gates", *Proc. of 3rd Symposium on Logic, Design and Learning*, Portland, Oregon, May 31st, 2000.

[13] R. Landauer, "Irreversibility and Heat Generation in the Computational Process" *IBM Journal of Research and Development*, **5**, pp.183-191, 1961.

[14] C. Moraga, "On a Property of the Chrestenson Spectrum", *Report No. AIUD/MVL/8102*, University of Dortmund, Dortmund, Germany, 1981.

[15] A. Muthukrishnan, and C. Stroud, "Multi-Valued Gates for Quantum Computation", *Phys. Rev*. A.62.052309, 2000.

[16] M. Nielsen and I. Chuang, *Quantum Computation and Quantum Information*, Cambridge University Press, 2000.

[17] S. Reddy, "Easily Testable Realizations of Logic Functions" *IEEE Trans. On Comp.*, **C-21**, pp.1183-1188, Nov. 1972.

[18] T. Sasao (editor), Representations of Discrete Functions, Kluwer 1996.

[19] C. P. Williams, and A. Gray, "*Automated Design of Quantum Circuits*", *Proc. of first NASA International Conference on Quantum Computing and Quantum Communications*, Palm Springs, CA, vol. 1509, Springer Verlag lecture notes in computer science, 1998.